

Characteristics of heat transfer and flow of Al_2O_3 /water nanofluid in a spiral-coil tube for turbulent pulsating flow

F. Ilami Doshmanziari¹ · A. E. Zohir² · H. Ramezani Kharvani¹ · D. Jalali-Vahid¹ · M. R. Kadivar³

Received: 2 October 2014 / Accepted: 27 July 2015 / Published online: 8 August 2015
© Springer-Verlag Berlin Heidelberg 2015

Abstract In the past two decades, enhancement of heat transfer characteristics of original fluid using nanofluids has been proposed by a large number of researchers. In this paper, an experimental study was carried out to investigate effect of pulsation on heat transfer of fluid flow inside a spiral-coil tube. In order to perform the experiments, a hot water reservoir tank was prepared and the spiral-coil was immersed horizontally inside the tank. Average temperature of the hot water bath was kept constant at 60 °C to establish a quiescent region of uniform temperature. The experiments were conducted in turbulent flow regime using distilled water and Al_2O_3 /water nanofluid at 0.5, 1, and 1.5 % particle volume concentration. Results showed that overall heat transfer coefficient of the base fluid flow increases by using nanofluid or pulsation into the base fluid flow up to 14 %. Heat transfer results also indicated that combination of the nanofluid and the pulsation into the fluid flow can increase significantly the overall heat transfer coefficient up to 23 %.

List of symbols

A Inside heat transfer area (m^2)
 C_p Specific heat capacity (J/kg K)
 D_i Inner diameter of tube (m)
 f Frequency (Hz)

K Thermal conductivity (W/m K)
 L Length of tube (m)
 \dot{m} Mass flow rate (kg/s)
 N Revolution per minute of the rotating valve spindle (rpm)
 Pe Peclet number
 Pr Prandtl number
 Q Heat transfer rate (W)
 r Inner radius of tube (m)
 R Radius of spiral coil (m)
 Re Reynolds number
 T Temperature (K)
 U Average overall heat transfer coefficient ($\text{W/m}^2 \text{K}$)
 V Average velocity of mean flow (m/s)
 Wo Womersly number, $Wo = \frac{D_i}{2} \sqrt{\frac{\omega}{\nu}}$

Greek letters

α Thermal diffusivity (m^2/s)
 μ Dynamic viscosity (kg/m s)
 ρ Density (kg/m^3)
 ν Kinematic viscosity (m^2/s)
 ω Angular pulsation frequency (1/s)
 ∞ Ambient medium
 φ Nanoparticle volumetric fraction

Superscript

– Average

Subscripts

ave Average
 i Inlet
 m Mean
 o Outlet
 pu Pulsated
 st Steady

✉ A. E. Zohir
alaa_sadegh@yahoo.com

¹ Faculty of Mechanical Engineering, Sahand University of Technology, Tabriz, Iran

² Mechanical Engineering Department, Tabbin Institute for Metallurgical Studies, Cairo, Egypt

³ Mechanical Engineering Department, Shiraz University, Shiraz, Iran

<i>P</i>	Nanoparticle
<i>nf</i>	Nanofluid
<i>f</i>	Base fluid

1 Introduction

Heat exchangers are devices that transfer thermal energy between two or more fluids at different temperatures. Heat exchangers are used in a wide variety of applications such as manufacturing industry, environmental engineering, air-conditioning, refrigeration, power production and space applications [1]. Thermal performance of heat exchangers can be significantly improved by numerous enhancement techniques which are classified into two general categories; passive techniques and active techniques [2, 3]. From the heat transfer enhancement point of view, a large quantity of research effort has been directed to heat transfer and flow characteristics in coiled tubes. Coiled tubes such as helical and spiral coils are used widely in variety of heat exchangers such as storage tanks, chemical reactors, agitated vessels, food processing, dairy, refrigeration and air conditioning. Generation of secondary flow due to centrifugal force, cross-sectional mixing enhancement and heat-mass transfer coefficients improvement are reasons for using these geometries. A review by Naphon and Wongwises [4] revealed that the most studies on heat transfer and flow characteristics in the coiled tubes have been devoted to helical-coil tubes whereas there are few studies for spiral-coil tubes. Using the nanoparticles under pulsating flow is a new idea for fluid flow mechanisms and heat transfer enhancement. Moreover, the pulsating flow has an advantage to prevent sedimentation of nanoparticles in the base fluid. Kubair and Kuloor [5] studied on heat transfer to Newtonian fluids in the coiled pipes in laminar flow. The experiments were based on two spirals that were enclosed in a steam chamber using glycerol solutions. They recommended a correlation for the Nusselt number as a function of Graetz number and average radius of curvature. Wijesundera et al. [6] investigated effect of the various design parameters on effectiveness of a spiral coil heat exchanger. Naphon and Suwagrai [7] investigated effects of curvature ratios on heat transfer and flow developments in the horizontal spirally coiled tubes. Three spirally coiled tubes with different curvature ratios were selected and the experiments were performed under constant wall temperature condition. They also simulated the turbulent flow and heat transfer characteristics by using the $k - \epsilon$ standard turbulence model. They reported that the average heat transfer coefficient increases with decreasing the curvature ratio.

On the other hand, the performance of heat exchangers can also be improved by the other heat transfer enhancement techniques. As an active technique,

pulsation in fluid flow is another method of heat transfer enhancement. Widespread studies have been allocated to pulsating flows and their associated heat transfer problems over the past decades [8–21]. Martinelli et al. [8] initiated the work on heat transfer characteristics of pulsating flow in 1943. They conducted the experiments on pulsating turbulent flow heat transfer in a vertical tube under uniform wall temperature boundary condition. The results showed that heat transfer reduces for pulsatile flow compared to steady flow at Reynolds numbers >4500 and increases at Reynolds number less than that. Havemann and Rao [9] performed a study on the heat transfer of pulsating turbulent flow in a horizontal pipe heated by steam. Reynolds number was ranged from 5000 to 35,000 while pulsation frequency was varied from 5 to 33 Hz. They reported that changes were negative below certain frequency and positive above it. Lemlich [10] investigated the effect of pulsation on heat transfer in a double pipe heat exchanger. Pulsating flow was produced by steady flow pump with a solenoid valve. The overall heat transfer coefficient of pulsating flow was approximately 80 % greater than the corresponding steady flow at Reynolds number of 2000 and pulsation frequency of 1.5 Hz. In another experiment carried out by Mamayev et al. [11] where air was passed through a vertical tube under constant wall heat flux condition. They reported that the maximum relative heat transfer coefficient was about 44 % at pulsation frequency of 12 Hz. Liao et al. [12] investigated an experiment to study the heat transfer in pulsating turbulent flow in a tube. Reynolds number was ranged from 3400 to 27,000 while pulsation frequencies were varied from 0.074 to 0.38 Hz. They found that the heat transfer coefficient without flow reversal was reduced about 20 %, but there was a 25 % increase in the heat transfer coefficient with flow reversal. Al-Haddad and Al-Binally [13] investigated experimentally heat transfer coefficient of air flowing through a heated circular tube in pulsating flow. Their results indicated that the heat transfer coefficient was increased by pulsation at high Reynolds number. Genin et al. [14] reported heat transfer characteristic of water flowing in a tube which was heated electrically in pulsating flow condition. In general, the effect of pulsating flow on the heat transfer coefficient was insignificant, in the range of investigated frequencies. Habib et al. [15] evaluated heat transfer characteristics of air in pulsating turbulent flow in a pipe. A rotating ball valve driven by a variable speed electric motor was used to impose flow pulsation while the pulsating mechanism located downstream of the tested pipe. They carried out their studies at a wide range of variables, Reynolds number of 8462–48,540 with the pulsation frequencies of 1–29.5 Hz. Their experimental results

showed about 50 % augmentation of mean Nusselt number at pulsation frequency between 13.9 and 29.5 Hz while Reynolds number of about 15,000 was considered. The results also showed that mean Nusselt number reduced at Reynolds number of more than 21,000 and this trend can be intensified by the increase of pulsation frequency. Simon et al. [16] studied heat transfer characteristics of pulsating laminar flow in curved tubes, employing a perturbation analysis. They evaluated their studies for a wide range of excitation parameters and Prandtl numbers. They reported that augmentation of time averaged Nusselt number is obvious at high Prandtl numbers, high excitation relative amplitudes, and low excitation frequencies. Based on the other research, Rabadi et al. [17] studied effects of pulsatile flow upon heat transfer characteristics in curved tubes under axially uniform heat flux boundary conditions with peripherally uniform wall temperature. The conflicting results were reported compared with the above-stated perturbation analysis. Chung and Hyun [18] solved numerically the time dependent incompressible Navier–Stokes equations over a range of Reynolds number, pulsation amplitude and frequency. They studied heat transfer and flow characteristics in a strongly curved pipe while the curvature ratio was considered small in the above-stated literature. They stated that the effect of pulsation on time and space-averaged Nusselt numbers was negative when the Womersley number was small while the change was insignificant at moderate and high Womersley number. Guo et al. [19] investigated heat transfer in fully developed pulsating turbulent flow in a helically coiled tube, experimentally. They reported that the secondary flow in helical coils with pulsating flow becomes so complicated that occur more than two circulations in a cross-section with the appearance of secondary flow reversal. Effect of pulsation on the heat transfer coefficient of air in a pipe, was studied experimentally by Zohir et al. [20]. They evaluated the Heat transfer characteristics under different conditions of Reynolds number, pulsation frequency, pulsation location and tube diameter for both laminar and turbulent pulsating pipe flows. They stated that the effect of pulsation on the heat transfer coefficient will improve the heat transfer if the pulsator valve becomes very closer to the entrance of the tested section. They obtained that the relative mean Nusselt number of downstream pulsation has better results than the upstream pulsation, at Reynolds number of 1366 and 1643. They also reported that, more improvement in heat transfer rate was obtained for a larger tube diameter at a Reynolds number range of 8000–12,000 with 1–10 Hz pulsation frequency. Zohir [21] investigated heat transfer characteristics of pulsating turbulent water flow in a double-pipe heat exchanger. The experiments were conducted

for both parallel and counter flows with upstream pulsation of different amplitudes. The result showed maximum increase of about 8 times in Nusselt number for the parallel flow and nearly 10 times for counter one.

In contrast, the conventional heat transfer fluids play an unpleasant role in heat transfer process because of their poor thermal properties. According to the heat transfer enhancement techniques [2, 3], based on the higher thermal conductivity of solids than liquids, additives such as solid particles can improve the thermal properties of the heat transfer fluids and therefore it would increase the efficiency of heat exchangers. The early research, suspension containing millimeter- and micrometer-sized particles was faced with the problem of poor suspension stability, due to the large size and high density of the particles. Addition of nanoscale solid particles to the conventional heat transfer fluids, to improve the thermal properties and the stability of a suspension, was proposed by Choi and Eastman [22]. In recent years, a great deal of research attention has been devoted to development of nanofluids for the engineering applications of heat transfer. An extensive review of the enhancement of forced convection heat transfer with nanofluids was provided by Kakaç and Pramuanjaroenkij [23]. Introduction of pulsation into nanofluids flow is a new idea in case of heat transfer enhancement techniques. Rahgoshay et al. [24] investigated pulsating flow of nanofluids through a pipe with isothermal walls, numerically. The results showed that by increasing both frequency and amplitude, a slight enhancement of Nusselt number obtained while more rate of heat transfer was observed by increasing Reynolds number and particles volume concentration. To evaluate effect of flow pulsation and nanoparticles on convection heat transfer over a wavy channel, Jafari et al. [25] carried out a study based on numerical simulation using the lattice Boltzmann method. The results indicated that the heat transfer rate increases using oscillating velocity and adding nanoparticles. Recently, Zhang et al. [26] investigated effect of vibration on forced convection heat transfer for SiO₂/water nanofluid. The results showed that the heat transfer coefficient can be enhanced by imposing a transverse vibration on the heat-transfer surface as well as adding nanoparticles. The results also indicated that using combination of two heat transfer enhancement methods, heat transfer performance is much better than that with either method alone.

Although a number of papers are currently available on the study of convective heat transfer of nanofluids in curved tubes, investigation on the heat transfer characteristics of nanofluids in spiral-coil tubes has not received considerable attention in the open literature. The purpose of the present research is to evaluate different heat transfer enhancement techniques on the performance of a

Table 1 Thermo-physical properties of alumina nanoparticles

d_p (nm)	ρ (kg/m ³)	C_p (J/kg K)	k (W/m K)
35	3890	880	40

horizontal spiral-coil tube (HSC-tube), to achieve higher thermal efficiency.

2 Details of experimental apparatus and procedure

2.1 Preparation and properties of nanofluid

Nanoparticles used in this study are Al₂O₃ with average diameter of 35 nm, from US Research Nanomaterials, Inc., Thermo-physical properties of alumina nanoparticles are shown in Table 1. The nanoparticles with volume concentrations of 0.5, 1 and 1.5 % are first diluted in deionized water and then are stirred by an ultrasonic bath at 160 W and 42 kHz for 4 h. No surfactant is used to stabilize the nanoparticles. After 24 h, the pH values of prepared nanofluids are between 5 and 6.2 using a digital pH meter (Metrohm, Model 827). The measured pH values are away from the isoelectric point of 9.2 for alumina nanoparticles. It shows that the dispersed nanoparticles were physically stable in the base fluid [27, 28].

Based on the physical principle of the mixture rule, calculation of density and heat capacity of the nanofluid are suggested by Pak and Cho [29] using the following relations:

$$\rho_{nf} = \varphi\rho_p + (1 - \varphi)\rho_f \quad (1)$$

$$C_{p,nf} = \frac{\varphi(\rho C_p)_p + (1 - \varphi)(\rho C_p)_f}{\rho_{nf}} \quad (2)$$

where the subscripts *nf*, *p* and *f* indicate nanofluid, nanoparticle and base fluid, respectively.

Corcione [30] proposed a correlation to estimates effective thermal conductivity of nanofluid by the following form:

$$\frac{K_{nf}}{K_f} = 1 + 4.4Re_p^{0.4}Pr_f^{0.66} \left(\frac{T}{T_{fr}} \right)^{10} \left(\frac{K_p}{K_f} \right)^{0.03} \varphi^{0.66} \quad (3)$$

where T_{fr} is the freezing point of the base liquid and Re_p is the nanoparticle Reynolds number calculated by the following form:

$$Re_p = \frac{\rho_f u_B d_p}{\mu_f} = \frac{2\rho_f K_B T}{\pi \mu_f^2 d_p} \quad (4)$$

where K_B and d_p are Boltzmann's constant (1.38066×10^{-23} J/K) and average diameter of nanoparticles, respectively. This equation is ranged from 10 to 150 nm for nanoparticles diameter, 0.2–9 % for volume concentration and from 294 to 324 K for temperature.

Other correlation of Corcione [30] proposed to estimate dynamic viscosity of nanofluid given by the following form:

$$\frac{\mu_{nf}}{\mu_f} = \frac{1}{1 - 34.87 \left(\frac{d_p}{d_f} \right)^{-0.3} \varphi^{1.03}} \quad (5)$$

where d_f is the equivalent diameter of a molecule of base fluid:

$$\begin{aligned} d_f &= \left(\frac{6M}{N\pi\rho_{f0}} \right)^{1/3} \\ &= \left(\frac{6 \times 0.01801528}{6.022 \times 10^{23} \times \pi \times 998.26} \right)^{1/3} = 3.85 \times 10^{-10} \text{ m} \quad (6) \end{aligned}$$

where M , N and ρ_{f0} are the molecular weight of the base fluid, Avogadro number and the mass density of the base fluid at temperature 293 K, respectively. This equation is restricted from 25 to 200 nm for nanoparticles diameter, 0.01–7.1 % for volume concentration and from 293 to 333 K for temperature.

2.2 Experimental apparatus

A schematic diagram of experimental apparatus is shown in Fig. 1. The experimental setup mainly comprises a fluid supply unit, pulsating mechanism, test section, data acquisition system and cooling unit. The fluid supply unit consists of a storage tank, pump and flow control valve. At a uniform temperature of 34 °C, cold fluid (nanofluid or base fluid) is pumped out of the storage tank by the peripheral electric pump (Lowara, Model PM16). The flow rate is controlled by the control valve and measured via collecting the fluid for a period of time by calibrated standard beaker and stopwatch. The pulsating mechanism includes an AC electric motor of 1 hp and 1500 rpm, a variable speed transmission and a rotating ball valve of 1/2 in. A power inverter is employed to change direct current 12 V to alternating current 220 V and can produce the input power to the AC electric motor. A coupling mechanism is designated and constructed as the transmission between the output of the AC motor and the rotating ball valve. Flow pulsation is introduced by the ball valve that can be adjusted manually to rotate with different frequencies. A digital tachometer (Autonics, Model MP5W) is used for measuring the rotation speed of the electric motor. The pulsator ball valve is located at the upstream of the test section while the pulsation amplitude is kept constant. The test section mainly

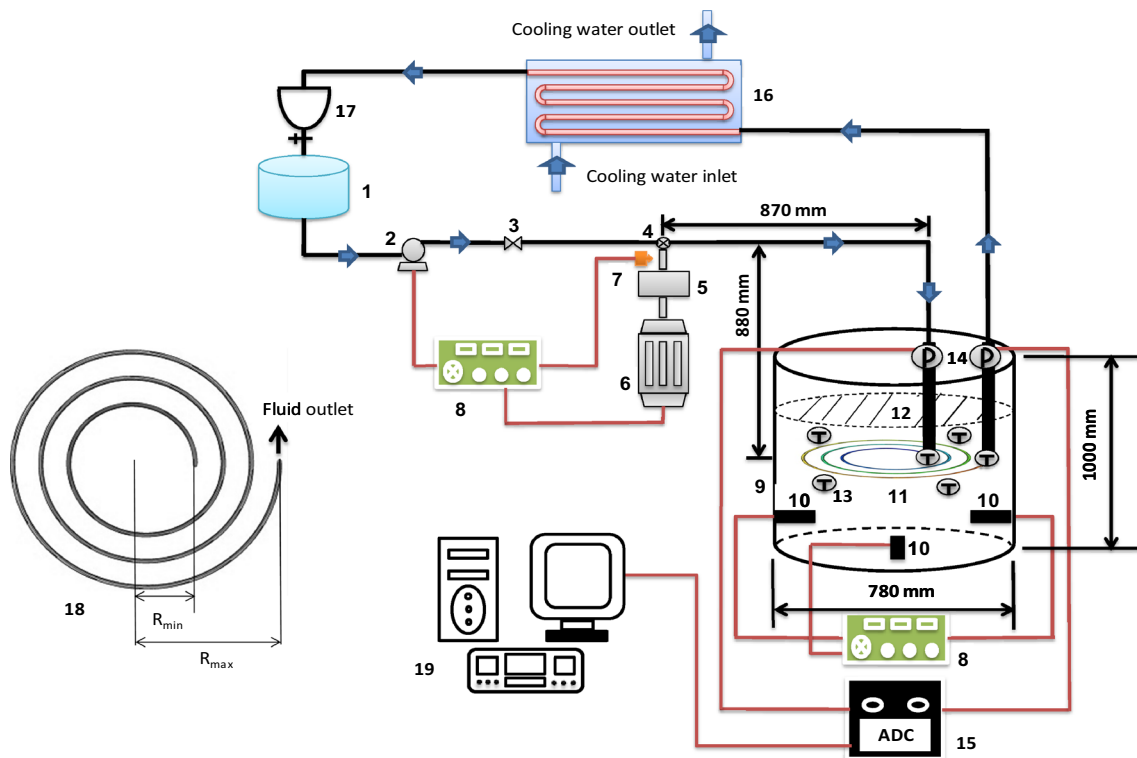


Fig. 1 Schematic diagram of the experimental apparatus. 1 Storage tank, 2, pump, 3 flow control valve, 4 pulsator ball valve, 5 coupling mechanism, 6 AC electric motor, 7 digital tachometer, 8 control unit, 9 hot water reservoir tank, 10 electrical heater, 11 HSC tube, 12 verti-

cal isolated tube, 13 RTD temperature sensor, 14 pressure transmitter, 15 analog-to-digital converter, 16 cooling unit, 17 flow rate measuring section, 18 the structure of HSC tube, 19 data acquisition system

Table 2 Dimensions of spiral-coil tube

Parameters	Dimensions
Inner diameter of tube (mm)	8.025
Outer diameter of tube (mm)	9.525
Innermost spiral coil radius (mm)	100
Outermost spiral coil radius (mm)	250
Length of spiral coil tube (mm)	3450
Pitch of spiral coil tube (mm)	50
Number of coil turns	3

consists of one hot water reservoir tank, three electrical heaters and one spiral-coil tube. The cylindrical reservoir tank is made of High-density polyethylene and it is used as a hot water bath. The hot water reservoir tank is insulated by two layers of 15 mm-thick polyurethane and 5 mm-thick galvanized polyurethane to minimize heat loss through its wall and diminish input power of electrical heaters. Two 2.5 kW electrical heaters and one electrical heater of 4 kW are installed at the bottom of the reservoir tank. The electrical heater of 4 kW is equipped with a power controller (Autonics Power Controller Spc1-35) to maintain the ambient hot water temperature at a constant value. The entrance

length for a laminar pulsating pipe flow to have fully developed flow can be calculated from [31]:

$$L/D_i = 0.049Re \quad (7)$$

where, D_i is the inner diameter of the tested tube. For turbulent flow, based on experimental data, the entrance length is much shorter than the corresponding ones for laminar flow. In this study, the experiments are performed in the turbulent regime. A vertical isolated copper tube with 8.025 mm inner diameter and length of 880 mm is attached to the entrance of the HSC tube. This length is long enough to ensure a fully developed flow at the entrance of the HSC tube. The spiral-coil tube is fabricated by copper alloy, UNS C12200, and it is immersed in the hot water horizontally. The HSC tube is also clamped by the reservoir tank wall to prevent vibration, induced by the flow pulsation. The dimensions of the HSC-tube are shown in Table 2. Four calibrated RTD temperature sensors of 0.1 °C accuracy are submerged in the hot water bath to measure the ambient temperature. In order to measure the temperature of the quiescent region accurately, the temperature sensors are placed in various locations of hot water bath. At the innermost coil turn of the HSC-tube, the cold fluid enters and flows along the tube. Two calibrated RTD temperature

sensors are installed into the flow to measure bulk temperatures of working fluid at the inlet and outlet of the HSC tube. The RTD temperature sensors are connected to a rotary selector switch and a digital temperature indicator. Two calibrated piezoresistive pressure transmitters (KELLER, SERIES 21 Y) are used to measure inlet and outlet pressure of the test section. An analog-to-digital converter (manufactured by TNM Electronics) with a resolution of 12 b is used as the interface between the pressure transmitters and data accumulation system, to convert transmitter analog signal to a digital number. Maximum sampling rate of the converter is 100 kHz that can be reduced to a desired number. Finally, 3125 samples/s are stored in the data accumulation system and therefore pressure drop measurements are fairly accurate. The cooling unit comprises a shell and tube heat exchanger in which cold water is used as cooling fluid.

2.3 Experimental procedure

Effect of the heat transfer enhancement techniques on the performance of a HSC tube are evaluated using an experimental procedure. In order to heat the quiescent water in reservoir tank, the electrical heaters are switched on and then the ambient temperature is controlled until average temperature of hot water reached 60 °C. Then, the electrical heaters of 2.5 kW are turned off while the ambient temperature is maintained at 60 °C by the electrical heater of 4 kW and the power controller during the experiment process. Base on the experimental program, the suspension is stirred by the ultrasonic bath for 1 h and then it is transferred to the test section immediately, to reduce nanoparticles sedimentation. Also, the pH value of nanofluid is measured during the experiment process, to ensure the stability of the nanofluid. For all pulsation frequencies, volume concentrations of nanoparticles and different cold fluid flow rates, the temperatures at the inlet and outlet of cold fluid are recorded, after achieving the steady state. The inlet and outlet pressure of the test section as a function of time are stored in the data accumulation system. The repeatability of measurements is observed in the repetitive run.

Table 3 Range of experimental variables

Experimental variables	Range
Volume flow rate (l/min)	2.5–5.5
Revolution per minute of the ball valve (rpm)	30–375
Particle volume concentration (%)	0.5–1.5
Reynolds number	8900–21,200
Peclet number	39,600–96,150
Womersly number	11.6–43.3

The range of experimental variables in the present study is given in Table 3.

3 Data reduction

The heat transfer rate absorbed by the cold fluid is calculated by:

$$Q = \dot{m}C_p(T_{m,o} - T_{m,i}) \quad (8)$$

where $T_{m,o}$ and $T_{m,i}$ are the outlet and inlet bulk temperature of the cold fluid, respectively. The thermo-physical properties of the cold fluid are evaluated at the mean bulk temperature for each test.

The average total heat transfer coefficient is defined as:

$$\bar{U} = \frac{Q}{A\Delta T_{lm}} \quad (9)$$

where A is the inside heat transfer area of the spiral-coil tube ($\pi D_i L$) and ΔT_{lm} is the logarithmic mean temperature difference, which can be obtained from:

$$\Delta T_{lm} = \frac{(T_\infty - T_{m,i}) - (T_\infty - T_{m,o})}{\ln \frac{(T_\infty - T_{m,i})}{(T_\infty - T_{m,o})}} \quad (10)$$

The average temperature of hot water is kept constant at 60 °C and can be obtained from:

$$T_\infty = \frac{T_1 + T_2 + T_3 + T_4}{4} \quad (11)$$

where T_1 , T_2 , T_3 and T_4 are the temperatures measured by the four sensors that are submerged in the quiescent region.

Substituting (8) and (10) into (9) and after some simplifications, the average overall heat transfer coefficient is determined from the following equation [32]:

$$\bar{U} = \frac{\dot{m}C_p}{\pi D_i L} \ln \left(\frac{T_\infty - T_{m,i}}{T_\infty - T_{m,o}} \right) \quad (12)$$

The flow is opened and closed twice for each revolution of the ball valve, so the frequency of pulsation can be calculated by the following form:

$$f = \frac{N \times 2}{60} \quad (13)$$

where N is the revolution per minute of the rotating valve spindle.

On the other hand, the angular pulsation frequency is obtained from:

$$\omega = 2\pi f \quad (14)$$

The Reynolds, Prandtl, Peclet and Womersly numbers are defined as follows:

$$Re = \frac{\rho \bar{V} D_i}{\mu} \quad (15)$$

$$Pr = \frac{\nu}{\alpha} = \frac{\mu C_p}{K} \quad (16)$$

$$Pe = Re \cdot Pr = \frac{\rho \bar{V} D_i C_p}{K} \quad (17)$$

$$Wo = \frac{D_i}{2} \sqrt{\frac{\omega}{\nu}} \quad (18)$$

where \bar{V} is the average velocity of the mean flow.

In the field of determining flow regime in pulsating flows, Hershey and Im [33] showed that transition from laminar to turbulent regime for pulsating flow of water in rigid tubes takes place at the Reynolds number of about 1500, that it is <2300 for steady flow. Clamen and Minton [34] stated that the pulsating flow becomes turbulent when the mean flow Reynolds number approaches to the critical Reynolds number of the steady pipe flow. Recently, Trip et al. [35] investigated the transitional regime of a sinusoidal pulsatile flow in a pipe using particle image velocimetry. They reported that pulsatile effects do not play a role in the transition regime, from laminar to turbulent flow. They also stated that for larger mean Reynolds numbers, the flow remains turbulent throughout the cycle. The critical Reynolds number for the fluid inside of the coil is calculated from the following relation [36]:

$$Re_{cr} = 2100 \left[1 + 12 \left(\frac{r}{R_{ave}} \right)^{0.5} \right] \quad (19)$$

where $R_{ave} = \frac{R_{min} + R_{max}}{2}$ and r are the average radius of spiral coil and inner radius of the tube, respectively. In the present work, transition occurs at the critical Reynolds number of about 5916.

4 Uncertainty analysis

The measurements are used for calculating some desired results of the experiment. Based on method of Kline and McClintock [37], the uncertainty analysis for the above experiments are carried out. The maximum uncertainties of average total heat transfer coefficient at lowest and highest flow rate are about 1.33 and 3.34 % for the nanofluid of 1 % volume concentration. The maximum uncertainties of Peclet number at lowest and highest flow rate are about 0.78 and 2.51 %. The uncertainty of Womersly number is 0.63 %.

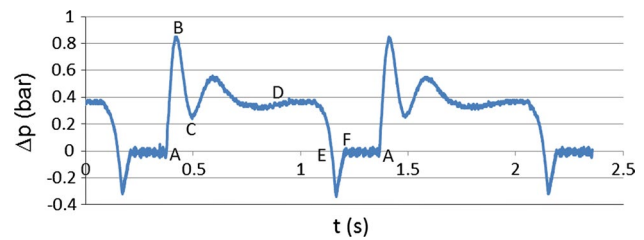


Fig. 2 Cyclic pressure drop for flow rate of 2.5 l/min ($f = 1$ Hz)

5 Results and discussion

In this study, 112 runs for different values of the experimental variables are carried out to evaluate the influence of flow pulsation and nanofluid on the performance of a HSC-tube.

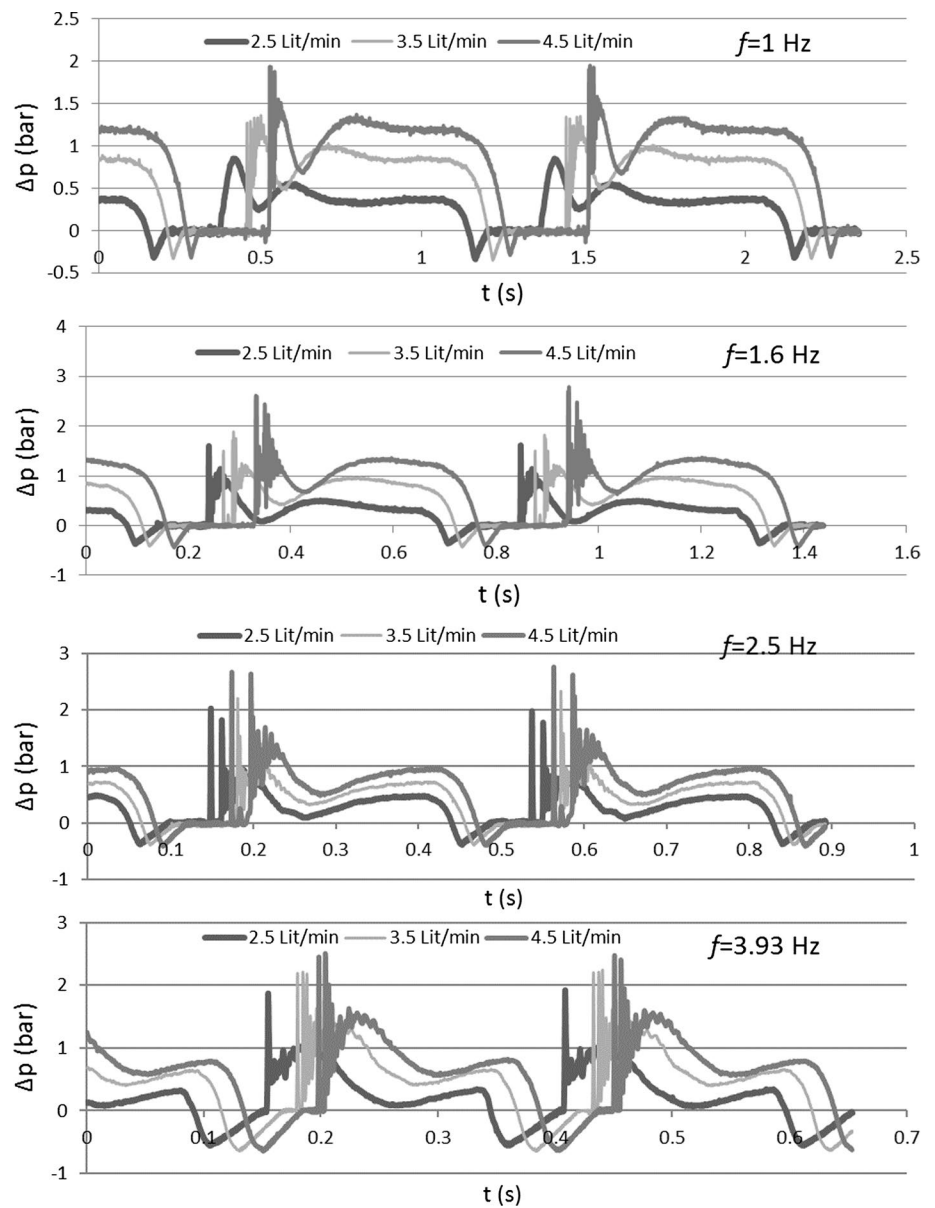
5.1 Flow considerations

In this research, hydrodynamic principles are performed to describe fluid flow behavior under different conditions inside the HSC-tube. The investigated values of cold fluid flow rates are 2.5, 3.5 and 4.5 l/min. The values of revolution per minute of the rotating ball valve spindle used in this study are 30, 48, 75, 118, 190, 235, 300 and 375 rpm. Therefore, the values of the pulsation frequency using Eq. (13) are 1, 1.6, 2.5, 3.93, 6.33, 7.83, 10 and 12.5 Hz.

For pulsation frequency of 1 Hz and flow rate of 2.5 l/min, cyclic pressure drop of the nanofluid of 0.5 % volume concentration in the test section is shown in Fig. 2. The cycle can be classified into two time steps: one is time step A–D, and the other is time step D–A. The first is when the pulsator ball valve opens and the second is when the pulsator ball valve closes. When the valve starts to open the passageway, the cold fluid enters the test section at a high velocity (A–B). However, because of the low velocity of the fluid at the downstream of the test section, the flow rate diminishes (B–C). Then, the valve opens entirely and the flow rate accelerates again (C–D). In the next time step, the valve starts to obstruct the fluid flow and the flow rate decreases (D–E). Afterwards, the fluid lacks sufficient momentum to overcome the pressure gradient and therefore, boundary layer separation occurs (the first zero-pressure drop). Henceforward, the flow reversal occurs until the flow approaches the second zero-pressure drop (E–F). Finally, the valve closes the passageway and the fluid flow stops for short time (F–A).

Figures 3 and 4 shows the cyclic pressure drop of the nanofluid of 0.5 % volume concentration in the test section at different pulsation frequencies for the flow rates of 2.5, 3.5 and 4.5 l/min. For pulsation frequencies of 1.6, 2.5

Fig. 3 Cyclic pressure drop for different flow rates ($f = 1, 1.6, 2.5$ and 3.93 Hz)



and 3.93 Hz, the flow fluid behavior is similar to the above-stated analysis as can be seen in Fig. 3. It can be clearly seen that for a given pulsation frequency, the pressure drop increases with increment of the flow rate while the flow behavior does not change. Figure 4 shows that at the high frequencies, the flow behavior approaches the behavior of a sinusoidal flow, the same as the ideal behavior of a pulsating flow. Figure 4 illustrates that at the start of the cycles, due to the fast rotation of the ball valve at the high frequencies, the intensity of the input flow decreases and also, the fluid flow does not stop at the end of the cycles, in opposite of the low frequencies.

The cyclic pressure drop of the nanofluids are represented in Fig. 5 for different volume concentrations

at pulsation frequency of 1 Hz and flow rate of 2.5 l/min. Addition of nanoparticles to the base fluid increases slightly the cyclic pressure drop of the nanofluid compared with that of the pure water. It is observed that the cyclic pressure drop of the nanofluid increases through increasing the nanoparticle concentration. For all the experiments, similar results can be considered.

5.2 Heat transfer results

The heat transfer results of various experiments considering different values of flow rates, pulsation frequency and nanoparticles volume concentration are represented and discussed in this section.

Fig. 4 Cyclic pressure drop for different flow rates ($f = 6.33, 7.83, 10$ and 12.5 Hz)

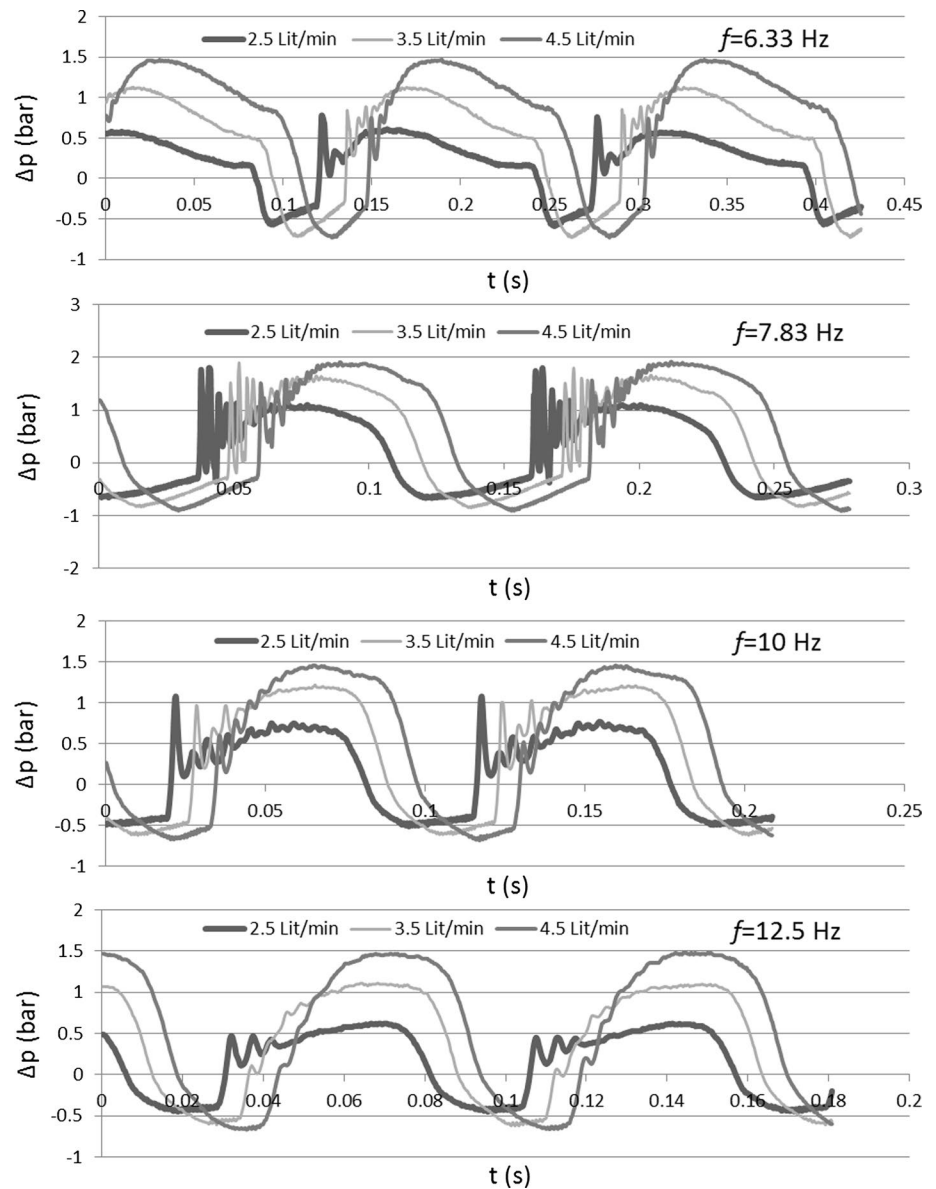
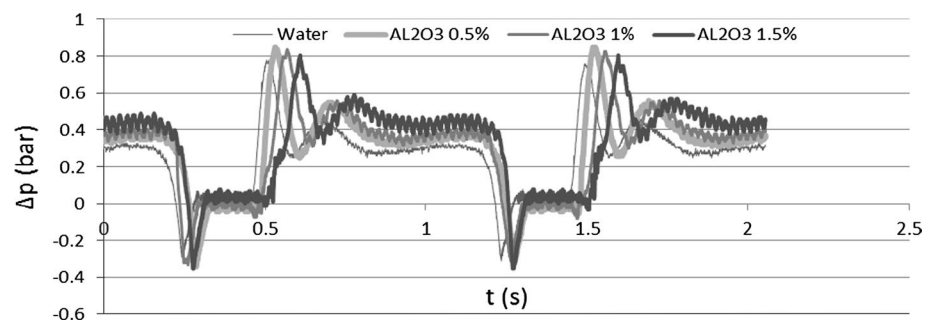


Fig. 5 Cyclic pressure drop of the nanofluids at different volume concentrations for flow rate of 2.5 l/min ($f = 1$ Hz)



5.2.1 Heat transfer in steady flow of nanofluid

Behavior of average total heat transfer coefficient with respect to Peclet number at different nanoparticle concentrations for the flow rates of $2.5, 3.5, 4.5$ and 5.5 l/min is

revealed in Fig. 6. As shown in this figure, the heat transfer coefficient of the nanofluid is higher than that of the base fluid (water) at a given Peclet number (flow rate). In the same way, it can be clearly seen that the heat transfer coefficient of the nanofluid increases with increasing the

Fig. 6 Average total heat transfer coefficient versus Peclet number at different nanoparticle concentrations

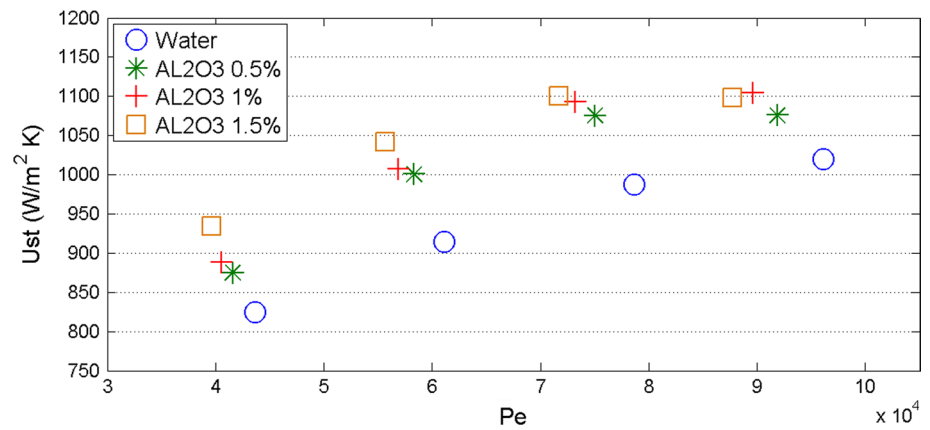
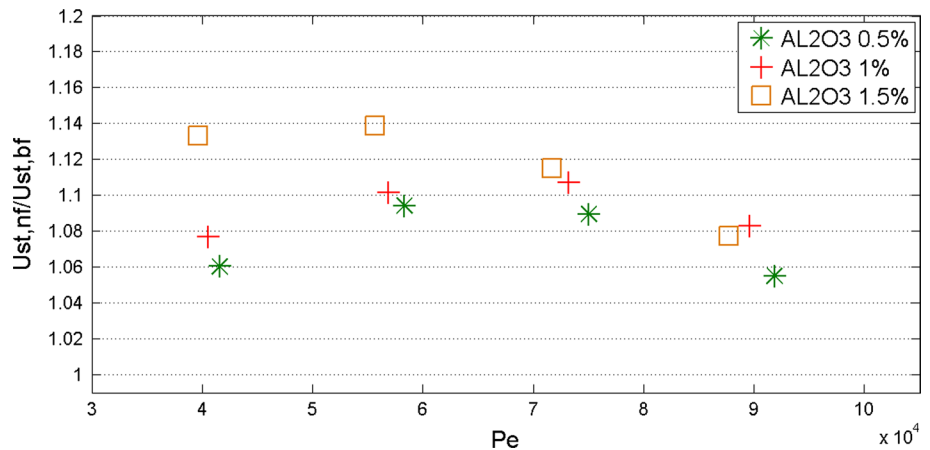


Fig. 7 Relative total heat transfer coefficient versus Peclet number at different nanoparticle concentrations



particle volume concentration as well as the Peclet number. Figure 7 displays that the enhancement of the total heat transfer coefficients are found to be about 6–14 %, in the range of investigated experiments. The increases in heat transfer with pulsation are due to the higher pulse intensity imparted to the flow through the whole pipe. The pulsation motion of the fluid results in a pressure gradient being created in the radial direction, thus affecting the boundary layer development. The increased rate of heat transfer in such flows is a consequence of the renewing and reducing the boundary layer thickness and increased resultant velocity. Energy transfer by nanoparticles dispersion, thermal conductivity enhancement, Brownian motion of particles, particle migration, reduction of boundary layer thickness and delay in boundary layer development can be the reasons for heat transfer enhancement of nanofluids [29, 38, 39].

Based on the literature survey, combination of two heat transfer enhancement techniques (utilizing coiled tubes and addition of nanoparticles to the base fluid) has a high capability to enhance heat transfer [40–43]. This may be attributed to reduction of nanoparticles sedimentation rate and cross-sectional mixing enhancement, due to the secondary

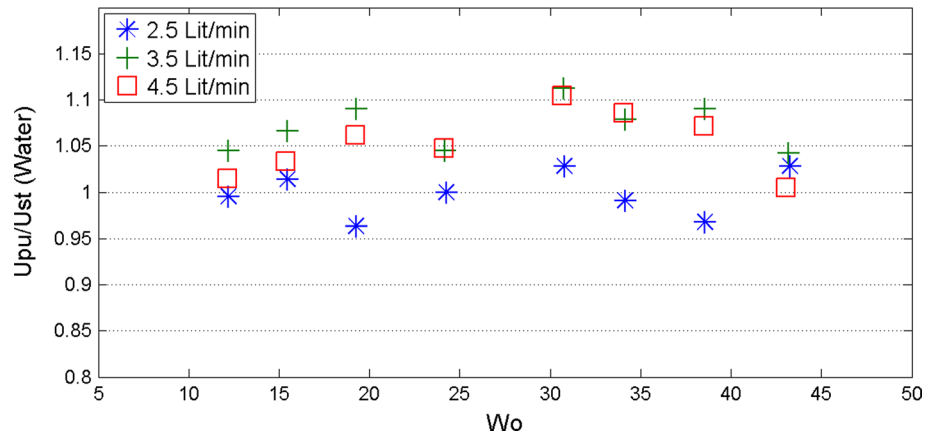
flow. It should be noted that the nanoparticles volume fraction does not have a direct effect on the secondary flow, also the cross-sectional distribution of solid nanoparticles is uniform because of the small size of the nanoparticles [44–47].

5.2.2 Heat transfer in pulsating flow of base fluid

Figure 8 depicts the variation of relative average total heat transfer coefficient versus Womersly number for different flow rates of the base fluid (deionized water). Relative average total heat transfer coefficient is defined as the ratio of the value of average total heat transfer coefficient for pulsated flow to the corresponding ones for steady flow at a same flow rate. A maximum enhancement in the relative heat transfer coefficient of about 11 % is observed at $Wo = 31$ for flow rate of 3.5 l/min while a maximum reduction of about 4 % is obtained at the operating conditions of $Wo = 18$ and flow rate of 2.5 l/min.

Generally speaking, a pulsating flow may enhance heat transfer by reducing thermal boundary layer thickness due to higher turbulence intensity. The heat transfer coefficients of such a flow are affected by several parameters

Fig. 8 Relative total heat transfer coefficient versus Womersly number for different flow rates (water)



such as inlet fluid temperature, boundary condition, Reynolds number, Prandtl number, type of pulsator, location of pulsator, pulsation frequency, pulsation amplitude, length to diameter ratio and secondary flow. Having higher velocity gradient at the tube wall, producing higher velocity at some moments, pressure gradient reversal during a period, producing forced circulation in the fluid and promoting the formation of eddies are the most important mechanisms of the heat transfer enhancement [10, 14, 48–50].

As mentioned before, based on the flow considerations, for the pulsation frequencies of 1, 1.6, 2.5 and 3.93 Hz, as shown in Fig. 3, at the start of these cycles, the cold fluid enters the test section at a high velocity and this leads to an increase in the heat transfer coefficient at these moments of the cycles. In contrast, the fluid flow stops at the end of the cycles and this leads to a decrease in the heat transfer coefficient. For the pulsation frequencies of 6.33, 7.83, 10 and 12.5 Hz, as shown in Fig. 4, at the start of these cycles, the intensity of the input flow decreases and this leads to a decrease in the heat transfer coefficient at these moments of the cycles. On the other hand, the fluid flow does not stop at the end of the cycles and this leads to an increase in the heat transfer coefficient at the corresponding moments when compared to that for the low frequencies. Based on the combination of the above opposite mentioned effects, the relative average total heat transfer can be enhanced or reduced, depending on the Womersly number range. As can be clearly observed from the Fig. 8, the effect of pulsating flow on the heat transfer coefficient is more significant at high values of Reynolds number (flow rate), due to higher turbulence intensity [9, 48, 51, 52]. Finally, the Secondary flow can be originated from the axial flow and therefore, it can be stated that intensification of the secondary flow and increasing temperature and velocity gradients near the outer wall at some moments of the cycle, radial and longitudinal mixing enhancement and the occurrence of secondary flow reversal play more important roles on the heat transfer improvement [17–19].

5.2.3 Comparison of the two heat transfer enhancement techniques

In the previous sections, two heat transfer enhancement techniques (additives for the base fluid including nanoparticles and introduction of pulsation into the base fluid flow) are separately investigated, to increase the thermal performance of the HSC-tube. The comparison between two heat transfer enhancement techniques shows that under the same experimental conditions, adding nanoparticles to the base fluid enhances the average total heat transfer coefficient for all experiments, however the introduction of pulsation into the base fluid flow decreases the average total heat transfer coefficient for the low flow rate, depending on the Womersly number range. For the nanofluids, the maximum increment in the heat transfer coefficient is observed at the low flow rates while the effect of pulsating flow on the heat transfer coefficient is more significant at high values of the flow rate. In general, the enhancements of the heat transfer rates for the HSC-tube using the nanofluid is greater than that using the pulsating flow, under the experimental conditions of this study.

5.2.4 Heat transfer in pulsating flow of nanofluid

In this section, the influence of combination of pulsation and nanofluid on the heat transfer rate is investigated. From Figs. 9, 10 and 11 shows the variation of relative average total heat transfer coefficient versus Womersly number at different flow rates of the $\text{Al}_2\text{O}_3/\text{water}$ nanofluid with nanoparticle volume fractions of 0.5, 1 and 1.5 %.

For flow rate of 2.5 l/min, it can be seen from Fig. 9 that the average total heat transfer coefficient of the nanofluid of 0.5 % volume concentration increases for pulsating flow compared to steady flow without pulsation at all Womersly numbers, especially at the high frequencies. An interesting observation in Fig. 9 is that at any value of Womersly number, the value of the relative average total heat transfer

Fig. 9 Relative total heat transfer coefficient versus Womersly number for different flow rates (Al_2O_3 0.5 %)

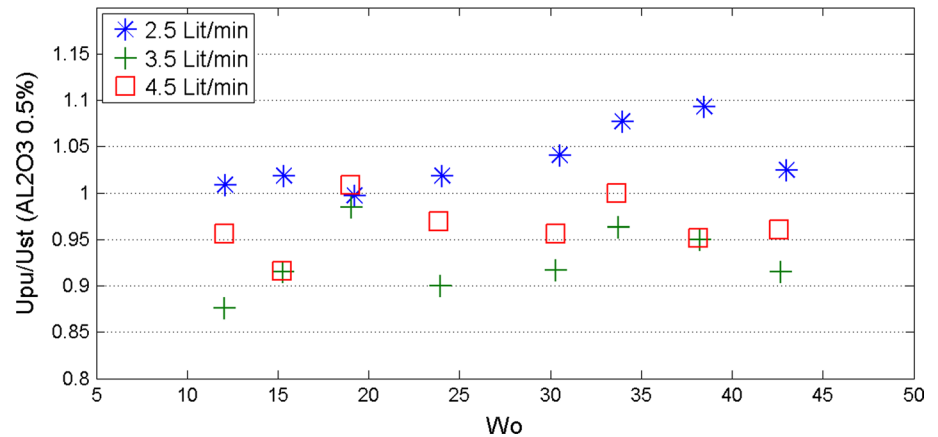


Fig. 10 Relative total heat transfer coefficient versus Womersly number for different flow rates (Al_2O_3 1 %)

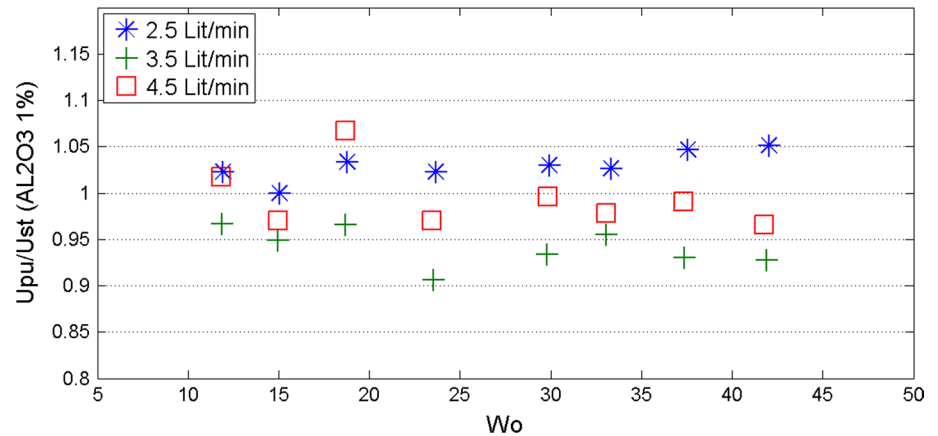
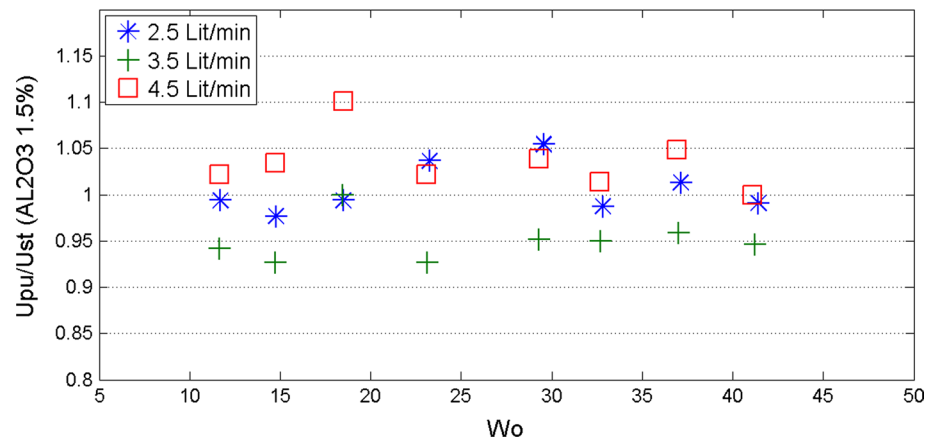


Fig. 11 Relative total heat transfer coefficient versus Womersly number for different flow rates (Al_2O_3 1.5 %)



coefficient is nearly less than unity at flow rates of 3.5 and 4.5 l/min.

The same trend for the relative average total heat transfer coefficient of the nanofluid of 1 % volume concentration as a function of Womersly number can be seen in Fig. 10, for flow rates of 2.5, 3.5 and 4.5 l/min. For flow rate of 2.5 l/min, there is a slight decline in the relative heat transfer coefficient of the nanofluid of 1 % volume concentration

compared with that of 0.5 % volume concentration, at the high frequencies. In contrast, there is a small growth in the relative heat transfer coefficient of the nanofluid of 1 % volume concentration compared with that of 0.5 % volume concentration, for flow rates of 3.5 and 4.5 l/min.

According to Figs. 9 and 10, a predictable tendency for the relative average total heat transfer coefficient of the nanofluid of 1.5 % volume concentration versus

Fig. 12 Relative total heat transfer coefficient versus Womersly number for flow rate of 2.5 l/min

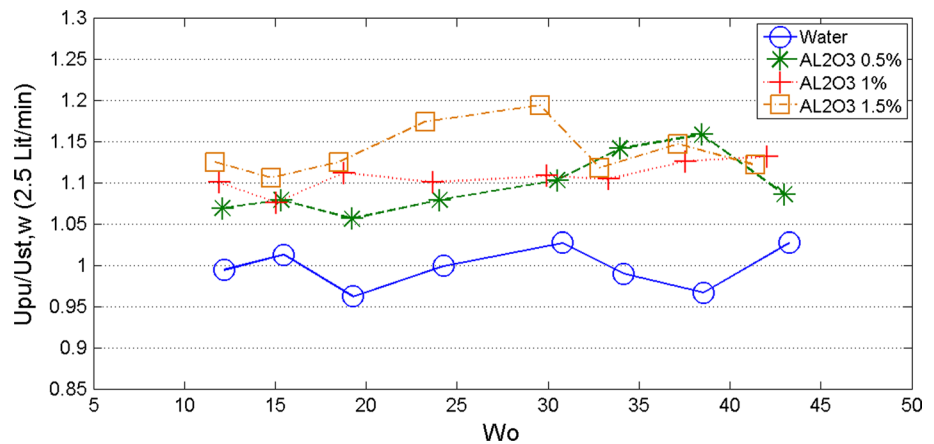
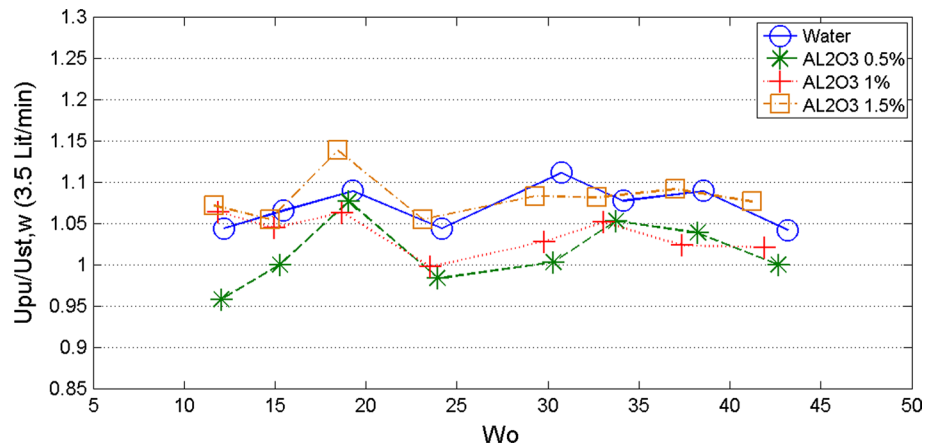


Fig. 13 Relative total heat transfer coefficient versus Womersly number for flow rate of 3.5 l/min



Womersly number can be observed in Fig. 11. For flow rate of 2.5 l/min, the heat transfer coefficient either increases or decreases over Womersly number values. A maximum enhancement in the relative heat transfer coefficient of about 6 % is observed at $Wo = 30$ while a maximum reduction of about 2 % is obtained at the operating conditions of $Wo = 15$. For flow rate of 3.5 l/min, the heat transfer coefficient of the nanofluid of 1.5 % volume concentration as well as that of 0.5 and 1 % volume concentrations decreases, affected by pulsed flow. For flow rate of 4.5 l/min, the heat transfer coefficient increases up to 10 % for pulsating flow compared to steady flow without pulsation at all pulsation frequencies.

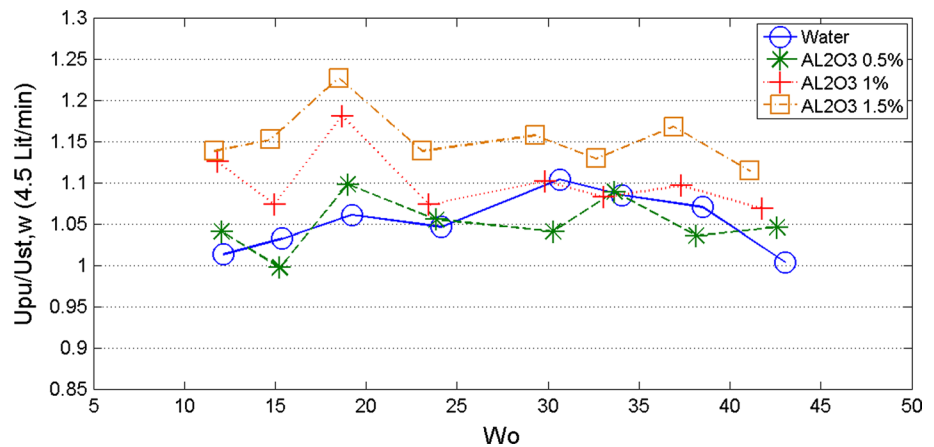
Pulsation in nanofluids is a new idea for enhancement of heat transfer. Furthermore, the pulsating flow has an advantage to prevent sedimentation of nanoparticles in the base fluid. Results show that the heat transfer performance increases significantly with increase in nanoparticle volume fraction and with the amplitude of pulsation while the pulsation frequencies have a slight effect. In the pulsating flow conditions the combined effect of pulsation and nanoparticles is favorable for the increasing the average total heat transfer coefficient when compared to the steady flow case.

Nevertheless, the average total heat transfer coefficient of the nanofluid decreases for pulsating flow compared to steady flow at some of the experiments, performed in this study. A possible reason for this trend might be because of an inappropriate distribution of the nanoparticles over the HSC-tube cross-section and hence a higher viscosity at the wall which leads to an increase in the boundary layer thickness and the corresponding thermal resistance. It must be stated that, the proposed mechanism is a hypothesis and further studies are needed to find out more details. Also, it is apparent from the figures that the relative average total heat transfer coefficient of the nanofluid is strongly affected by flow rate, i.e., at the flow rate of 3.5 l/min, the relative heat transfer coefficient of the nanofluid is not sensitive to the nanoparticles concentration and is constantly less than unity.

5.2.5 Introduction of pulsation into fluid flow to enhance heat transfer

From Figs. 12, 13 and 14 shows the variation of the average total heat transfer coefficient of the working fluid (both the nanofluid and the base fluid) with pulsating flow compared

Fig. 14 Relative total heat transfer coefficient versus Womersley number for flow rate of 4.5 l/min



with that of the base fluid with steady flow, under different experimental conditions. Therefore, relative average total heat transfer coefficient is defined as the ratio of the value of average total heat transfer coefficient of the working fluid for pulsated flow to the corresponding ones for steady flow of the base fluid, at a same flow rate.

For flow rate of 2.5 l/min, it is clear from Fig. 12 that in the pulsating flow, application of the nanofluid instead of the base fluid increases the heat transfer coefficient significantly. According to this figure, contrary to the high frequencies, the relative heat transfer coefficient of the nanofluid increases with increasing the particle volume concentration at the low frequencies. The relative heat transfer coefficients increase up to 16, 13 and 20 % at $Wo = 39, 42$ and 29 and for the nanofluid with nanoparticle volume fractions of 0.5, 1 and 1.5 %, respectively. While a maximum enhancement of about 3 % is obtained at the operating conditions of $Wo = 31$ and 43 for the base fluid.

For flow rate of 3.5 l/min, the results indicate that, the relative heat transfer coefficient of the nanofluids does not increase when compared to that of the results obtained using the base fluid as can be seen from Fig. 13. For the nanofluid of 0.5 % volume concentration, it is possible that the relative heat transfer coefficient decreases at the low range of the pulsation frequencies. A maximum enhancement in the relative heat transfer coefficient of about 14 % is observed at $Wo = 18$ for the nanofluid with nanoparticle volume fraction 1.5 % while a maximum increase of about 11 % is obtained at the operating conditions of $Wo = 31$ for the base fluid.

According to Fig. 14, for flow rate of 4.5 l/min, at the low range of the pulsation frequencies, application of the nanofluid instead of the base fluid increases the relative heat transfer coefficient significantly when compared to that for the high frequencies. The relative heat transfer coefficients increase up to 10, 18 and 23 % at $Wo = 19$ and for the nanofluid with nanoparticle volume fractions of 0.5, 1 and 1.5 %, respectively. While a maximum enhancement

of about 11 % is obtained at the operating condition of $Wo = 31$ for the base fluid.

As an overall trend, it is obvious from the figures that the beneficial effect of increasing the concentration of nanoparticles on the heat transfer is more effective at the low range of the pulsation frequencies, for a given flow rate.

6 Conclusion

This research has provided an experimental investigation of the effects of pulsation on the heat transfer and flow characteristics of Al_2O_3 /water nanofluid under turbulent flow conditions in a spiral-coil tube. The experiments are performed in a quiescent region of uniform temperature. The effects of flow rate, pulsation frequency and nanoparticles volume concentration are investigated. The addition of nanoparticles to the base fluid and introduction of pulsation into the base fluid flow can increase the performance of a HSC-tube, to achieve higher thermal efficiency. The heat transfer of the base fluid flow increases by using nanofluid or introduction of pulsation into the base fluid flow. Pulsation can increase or decrease the heat transfer rates of the nanofluid flows according to the pulsation frequency, flow rate and nanofluid concentration. It must be stated that, the temperature of the inlet fluid is constant at $34\text{ }^\circ\text{C}$ for all the experiments. Besides, the inside heat transfer area of the HSC-tube ($\pi D_i L$) is 0.087 m. It might be expected that, better results can be obtained with decreasing the temperature of the inlet fluid and/or increasing the inside heat transfer area of the HSC-tube, in the studied range of this research. The overall heat transfer coefficient of the base fluid flow increases by using nanofluid or pulsation up to 14 %. The combination of the nanofluid and the pulsation into the fluid flow can increase significantly the overall heat transfer coefficient up to 23 %. Pulsation in the nanofluid flows is more effective to achieve higher thermal efficiency.

Acknowledgments The authors would like to thank Iran Nanotechnology Initiative Council (INIC) for their financial support.

References

- Kakaç S, Pramuanjaroenkij A, Liu H (2012) Heat exchangers: selection, rating, and thermal design. CRC Press, Boca Raton
- Bergles A (1988) Some perspectives on enhanced heat transfer—second-generation heat transfer technology. *J Heat Transf* 110:1082–1096
- Bergles AE (1998) Techniques to enhance heat transfer. In: Rohsenow WM, Hartnett JP, Cho YI (eds) *Handbook of Heat Transfer*. McGraw-Hill, New York, pp 11.1–11.76
- Naphon P, Wongwiset S (2006) A review of flow and heat transfer characteristics in curved tubes. *Renew Sustain Energy Rev* 10:463–490
- Kubair V, Kuloor N (1966) Heat transfer to Newtonian fluids in coiled pipes in laminar flow. *Int J Heat Mass Transf* 9:63–75
- Wijesundera N, Ho J, Rajasekar S (1996) The effectiveness of a spiral coil heat exchanger. *Int Commun Heat Mass Transf* 23:623–631
- Naphon P, Suwagrai J (2007) Effect of curvature ratios on the heat transfer and flow developments in the horizontal spirally coiled tubes. *Int J Heat Mass Transf* 50:444–451
- Martinelli R, Boelter LMK, Weinberg E, Yakahi S (1943) Heat transfer to a fluid flowing periodically at low frequencies in a vertical tube. *Trans ASME* 65:789–798
- Havemann H, Rao NN (1954) Heat transfer in pulsating flow. *Nature* 7(4418):41
- Lemlich R (1961) Vibration and pulsation boost heat transfer. *Chem Eng* 68:171–176
- Mamayev V, Nosov V, Syromyatnikov N (1976) Investigation of heat transfer in pulsed flow of air in pipes. *Heat Transf Sov Res* 8:111–116
- Liao N, Wang C, Hong J (1985) An investigation of heat transfer in pulsating turbulent pipe flow. In: *The 23rd national heat transfer conference in fundamentals of forced and mixed convection*, Denver, CO, USA, pp 4–7
- Al-Haddad AA, Al-Binaly N (1989) Prediction of heat transfer coefficient in pulsating flow. *Int J Heat Fluid Flow* 10:131–133
- Genin L, Koval A, Manchka S, Sviridov V (1992) Hydrodynamics and heat transfer with pulsating fluid flow in tubes. *Therm Eng* 39:251–255
- Habib M, Attya A, Said S, Eid A, Aly A (2004) Heat transfer characteristics and Nusselt number correlation of turbulent pulsating pipe air flows. *Heat Mass Transf* 40:307–318
- Simon H, Chang M, Chow J (1977) Heat transfer in curved tubes with pulsatile, fully developed, laminar flows. *J Heat Transf* 99:590–595
- Rabadi N, Chow J, Simon H (1982) Heat transfer in curved tubes with pulsating flow. *Int J Heat Mass Transf* 25:195–203
- Chung JH, Hyun JM (1994) Heat transfer from a fully-developed pulsating flow in a curved pipe. *Int J Heat Mass Transf* 37:43–52
- Guo L, Chen X, Feng Z, Bai B (1998) Transient convective heat transfer in a helical coiled tube with pulsatile fully developed turbulent flow. *Int J Heat Mass Transf* 41:2867–2875
- Zohir A, Habib M, Attya A, Eid A (2006) An experimental investigation of heat transfer to pulsating pipe air flow with different amplitudes. *Heat Mass Transf* 42:625–635
- Zohir A (2012) Heat transfer characteristics in a heat exchanger for turbulent pulsating water flow with different amplitudes. *J Am Sci* 8:241–250
- Choi SU, Eastman J (1995) Enhancing thermal conductivity of fluids with nanoparticles. Argonne National Lab, IL, USA
- Kakaç S, Pramuanjaroenkij A (2009) Review of convective heat transfer enhancement with nanofluids. *Int J Heat Mass Transf* 52(13–14):3187–3196
- Rahgoshay M, Ranjbar A, Ramiar A (2012) Laminar pulsating flow of nanofluids in a circular tube with isothermal wall. *Int Commun Heat Mass Transf* 39:463–469
- Jafari M, Farhadi M, Sedighi K (2014) Heat transfer enhancement in a corrugated channel using oscillating flow and nanoparticles: an LBM approach. *Numer Heat Transf Part A Appl* 65:601–626
- Zhang L, Lv J, Bai M, Guo D (2015) Effect of vibration on forced convection heat transfer for SiO₂–water nanofluids. *Heat Transf Eng* 36(5):452–461
- Das SK, Putra N, Thiesen P, Roetzel W (2003) Temperature dependence of thermal conductivity enhancement for nanofluids. *J Heat Transf* 125:567–574
- Putra N, Thiesen P, Roetzel W (2003) Temperature dependence of thermal conductivity enhancement for nanofluids. *J Heat Transf* 125:567–574
- Pak BC, Cho YI (1998) Hydrodynamic and heat transfer study of dispersed fluids with submicron metallic oxide particles. *Exp Heat Transf Int J* 11:151–170
- Corcione M (2011) Empirical correlating equations for predicting the effective thermal conductivity and dynamic viscosity of nanofluids. *Energy Convers Manag* 52:789–793
- Özdiñç Çarpınlioğlu M, Yaşar Gündoğdu M (2001) A critical review on pulsatile pipe flow studies directing towards future research topics. *Flow Meas Instrum* 12:163–174
- Incropera FP, Lavine AS, DeWitt DP (2011) *Fundamentals of heat and mass transfer*. Wiley, Hoboken
- Hershey D, Im CS (1968) Critical Reynolds number for sinusoidal flow of water in rigid tubes. *AIChE J* 14:807–809
- Clamen M, Minton P (1977) An experimental investigation of flow in an oscillating pipe. *J Fluid Mech* 81:421–431
- Trip R, Kuik D, Westerweel J, Poelma C (2012) An experimental study of transitional pulsatile pipe flow. *Phys Fluids* 24:014103
- Srinivasan P, Nandapurkar S, Holland F (1970) Friction factors for coils. *Trans Inst Chem Eng* 48:T156–T161
- Kline SJ, McClintock F (1953) Describing uncertainties in single-sample experiments. *Mech Eng* 75:3–8
- Wen D, Ding Y (2004) Experimental investigation into convective heat transfer of nanofluids at the entrance region under laminar flow conditions. *Int J Heat Mass Transf* 47:5181–5188
- Chen H, Yang W, He Y, Ding Y, Zhang L, Tan C, Lapkin AA, Bavykin DV (2008) Heat transfer and flow behaviour of aqueous suspensions of titanate nanotubes (nanofluids). *Powder Technol* 183:63–72
- Akhavan-Behabadi M, Pakdaman MF, Ghazvini M (2012) Experimental investigation on the convective heat transfer of nanofluid flow inside vertical helically coiled tubes under uniform wall temperature condition. *Int Commun Heat Mass Transf* 39:556–564
- Kahani M, Heris SZ, Mousavi S (2013) Effects of curvature ratio and coil pitch spacing on heat transfer performance of Al₂O₃/water nanofluid laminar flow through helical coils. *J Dispers Sci Technol* 34:1704–1712
- Kahani M, Zeinali Heris S, Mousavi S (2013) Comparative study between metal oxide nanopowders on thermal characteristics of nanofluid flow through helical coils. *Powder Technol* 246:82–92
- Kahani M, Heris SZ, Mousavi S (2014) Experimental investigation of TiO₂/water nanofluid laminar forced convective heat transfer through helical coiled tube. *Heat Mass Transf* 50(11):1563–1573
- Akbarinia A, Behzadmehr A (2007) Numerical study of laminar mixed convection of a nanofluid in horizontal curved tubes. *Appl Therm Eng* 27:1327–1337

45. Akbarinia A (2008) Impacts of nanofluid flow on skin friction factor and Nusselt number in curved tubes with constant mass flow. *Int J Heat Fluid Flow* 29:229–241
46. Akbarinia A, Laur R (2009) Investigating the diameter of solid particles effects on a laminar nanofluid flow in a curved tube using a two phase approach. *Int J Heat Fluid Flow* 30:706–714
47. Ghaffari O, Behzadmehr A, Ajam H (2010) Turbulent mixed convection of a nanofluid in a horizontal curved tube using a two-phase approach. *Int Commun Heat Mass Transf* 37:1551–1558
48. West F, Taylor A (1952) The effect of pulsations on heat transfer-turbulent flow of water inside tubes. *Chem Eng Prog* 48:39–43
49. Karamercan OE, Gainer JL (1979) The effect of pulsations on heat transfer. *Ind Eng Chem Fundam* 18:11–15
50. Wang X, Zhang N (2005) Numerical analysis of heat transfer in pulsating turbulent flow in a pipe. *Int J Heat Mass Transf* 48:3957–3970
51. Keil R, Baird M (1971) Enhancement of heat transfer by flow pulsation. *Ind Eng Chem Process Des Dev* 10:473–478
52. Zohir A (2011) The influence of pulsation on heat transfer in a heat exchanger for parallel and counter water flows. *New York Sci J* 4(6):61–71